International Journal of Civil Engineering

Geotechnical Engineering

An investigation on effect of inclusions on heterogeneity of stress, excess pore pressure and strain distribution in composite soils

J. Jalili[1,*], M. K. Jafari[2], A. Shafiee[3], J. Koseki[4], T. Sato[5]

Received: January 2011, Revised: May 2011, Accepted: August 2011

Abstract

A series of tests and also numerical analyses were conducted to explore the mechanical behavior of a mixture of coarse gravel-size particles floating in a matrix of silt, sand or clay. The research is a step forward in an ongoing investigation on behavior of composite clay, which is used as the core material of some large embankment dams all over the world. After providing the reader with an overall image about behavior of such materials through the literature, the paper focuses on a predominant feature of the composite soil behavior: increase of non-deformable solid inclusions in a mixture leads to formation of heterogeneity of stress field, excess pore water pressure and strain distribution along the specimens. This paper mainly probes formation of such heterogeneity by the aid of special experiments and also numerical analyses. In addition to loading details, it is clarified through the paper that position of inclusions relative to loading direction also affects heterogeneity of stress/strain and excess pore water pressure distribution through the mixture. Despite the former, the latter redistributes with a rate proportional to material hydraulic conductivity.

Keywords: Composite soil, Mixed material, Heterogeneity, Torsional hollow cylinder, Cyclic triaxial, Finite element analysis

1. Introduction

Natural fine-grained soils normally contain a significant proportion of larger bulky particles. There are also slopes made of glacial tills, mudflows or debris flows, consisting of a mixture of large particles and a soft matrix of fines. In such mixtures, which have been used as impervious material for the core of embankments, or as deposit liners, it is believed that the finer fraction would provide sealing while the coarser grains would make the material less compressible and stronger in terms of shear strength.

Focusing on trend of excess pore water pressure development in such materials, an extensive research has been conducted on cyclic and post-cyclic behavior of composite clays [1]. Based on the findings of these researches, the prominent feature of composite clay behavior is the increase of clay-fraction deformation by the increase of inclusions as the non-deformable solid fraction of the mixture, especially under strain-controlled loadings. Consequently, as grains volume fraction of the mixture is raised, larger extents of excess pore water pressure (EPWP) may be generated during both monotonic and cyclic loadings.

The main goal of the current investigation is to observe the heterogeneity of effective stress/pore pressure and strain throughout the specimen, and in a wider range of matrix materials, by the aid of some experiments and also numerical analyses. For the testing purposes, a joint research was conducted between International Institute of Earthquake Engineering and Seismology (IIEES), Iran and Institute of Industrial Science, the University of Tokyo, Japan, making use of medium-size specimens in torsional hollow cylinder and cyclic triaxial apparatus, with two or one miniature pressure-transducer(s) inside the specimen. The numerical analysis was also performed by Plaxis 3D and 2D finite element codes.

The paper is prepared mainly in three parts: First part provides the reader with a brief and relatively thorough research background; second part is devoted to testing method and subsequent findings; and third part presents the analytical results. Finally a conclusion is made from the results.

* *Corresponding Author: jafari@iiees.ac.ir*
1 Ph.D. candidate, Geotechnical research center, International Institute of Earthquake Engineering and Seismology
2 Professor, Geotechnical research center, International Institute of Earthquake Engineering and Seismology
3 Assisstant professor, Geotechnical research center, International Institute of Earthquake Engineering and Seismology
4 Professor, Geotechnical Engineering Laboratory, Institute of Industrial Science, The University of Tokyo
5 Private sector collaborative researcher, , Geotechnical Engineering Laboratory, Institute of Industrial Science, The University of Tokyo

2. Research background

As composite soils are frequently found in nature, their physical (e.g. compaction characteristics and permeability) and mechanical (e.g. monotonic and cyclic shear resistance) properties have been matters of concern, though not as much as those of pure sand, silt or clay soils. As the main focus of this paper is on a mechanical aspect of mixed-soil behavior, only some relevant studies are reviewed here. Readers may find more extensive reviews concerning physical properties also, in the references which will be pointed out through the paper.

2.1. Near-field and Far-field in mixtures

Fragaszy et al. (1992) divided clay-aggregate mixtures to floating case (in which grains have no contact) and non-floating case (in which grains touch each other), as shown in Fig. 1a. With the assumption that in a floating case large particles have no significant effect on shear strength and deformation characteristics of the mixture, they prepared model samples of matrix portion alone, with a density similar to what exists within the prototype soil away from the particles. Results of triaxial tests on large prototype and model samples showed the similar peak shear strength, and also similar stress-strain and volumetric strain-axial strain behavior up to the peak shear stress.

In the current study, the concept of "near-" and "far-field" has been preferred to describe different zones of the mixture, in subsequent parts of the paper.

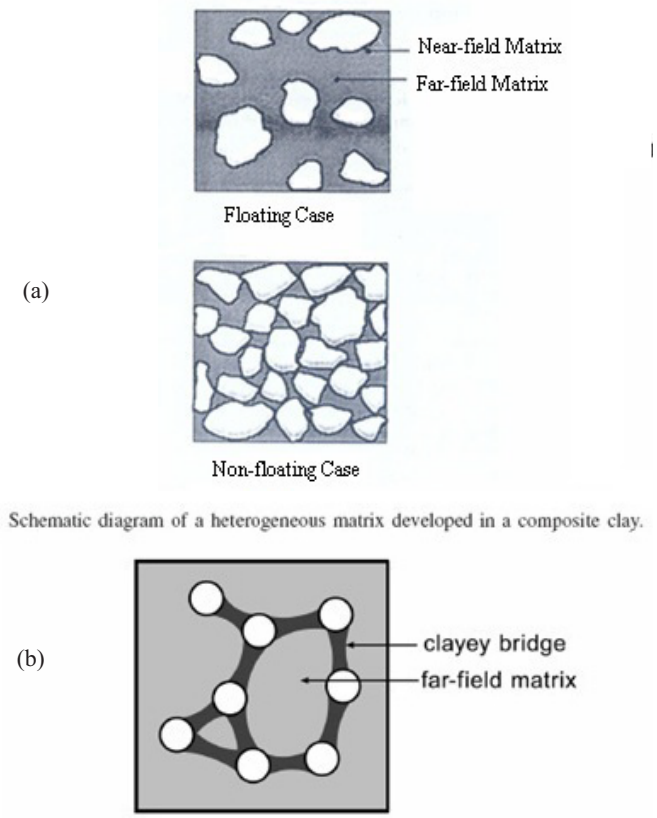

Fig. 1. Schematic of a) near-field and far-field matrixes (Fragaszy et al., 1992) b) clay bridge and far-field matrix [1]

2.2. Grain content

Contribution of mixture components to the overall material behavior is another issue explored by different authors. Vallejo and Mawby (2000) reported a review of shear

strength measurements carried out on mixture proportions that varied between 0 and 100% of either gravel or sand (representing the granular phase of the mixtures) and clay, by various researchers. The average of the reported findings and those measured by the authors were nearly consistent, i.e. when the weight concentration of the grains exceeds 75%, the behavior of the mixture is governed by the grains, and when it is less than 40%, clay content has the predominant role. Both clay and grains take part in shear strength of the mixtures with grain content between the mentioned limits. They also followed similar trend of tests in measuring void ratio, using sand and clay, and concluded that the porosity of the mixture was related to the same percentages of sand in the mixtures as those of shear strength. Kumar and Muir Wood (1999) and Muir Wood and Kumar (2000) also had similar conclusions, after performing fall cone, one dimensional compression and triaxial tests on mixtures of kaolin clay and fine gravel or coarse sand.

Based on these findings, granule volume content of the mixture during experiments of the current study were considered equal to or above 40%, though the main focus is on EPWP development, which is affected by any percentage of the granule content.

2.3. Heterogeneity of mixture response

To investigate mechanical behavior of clay-aggregate mixtures especially in the aspect of EPWP development, Jafari and Shafiee (1998; 2004) commenced a pioneering extensive research on this material, by conducting several monotonic and cyclic triaxial tests. The effect of granular material content, number of cycles, cyclic strain amplitude, grain size and confining pressure on the behavior of the mixture were evaluated. Soroush and Soltani-Jigheh (2009) also explored the same material, focusing mainly on its post-cyclic behavior, and observed the same tendency as the former one. For the sake of brevity, readers are referred to Soroush and Soltani-Jigheh (2009) to review the literature in this regard i.e. the effect of grain content on static and cyclic shear strength of mixed clay soils. The prominent feature revealed by these investigations is increase of average EPWP with increase of aggregate content, especially in higher confining pressures and strain amplitudes. This is mainly devoted to higher strain magnitudes exerted to the clay part of the mixtures (assuming no deformation for the solid inclusions) in comparison with pure clay specimens, under the same strain amplitudes.

Heterogeneity of the matrix soil of the mixture which is mainly induced during compaction and consolidation of the specimen was the other observed trend of behavior in these studies. Due to existence of granular inclusions, those regions which are between two adjacent grains (clay bridge, Fig. 1b) are believed to be highly compacted and consolidated, despite the so-called far-field areas. This local difference of density would be the source of further heterogeneous effective stress

and EPWP distribution in subsequent cycles of strain. However, based on the permeability of the matrix soil, the EPWP heterogeneity tends to uniformity by decrease of loading frequency, as a result of pore water pressure redistribution.

In the above mentioned studies, the only evidences of such heterogeneity was measurement of pore water pressure at both ends of the specimen, and also some scanning electron microscope photographs of horizontal sections of the specimen after the tests [1, 8]. However, in the reviewed literature, there is no record of any measurement inside the specimens while loading, to capture formation of such heterogeneous fields of stress more quantitatively. This lack of evidence was the main reason of the current study, which is seeking heterogeneity of stress (including EPWP) and strain distribution inside the specimens.

2.4. Analytical study of mixture behavior

In the field of analytical studies on mixed materials, Gutierrez (2002; 2003) used volume fraction (or percentage by weight in some cases) of each constituent of a mixture to determine the effective average properties of the mixed material from the individual properties of the constituents (mixture theory). It is assumed in this theory that each constituent of the mixture simultaneously occupies the same region in space at a macroscopic scale. Void ratio and normalized cyclic undrained shear strength of sand and silt mixtures evaluated by this theory were consistent with findings of the previous experiment results. Wang et al. (2002) also used a homogenization method to predict some characteristic parameters such as Young's modulus, Duncan-Chang model parameters or strength parameter for mixed soils and composite ground, which showed good agreement with measured data. Wickland et al. (2006) predicted mixture compressibility from mixture ratio and properties of the parent constituents as well.

Wood and Kumar (2000) however, compared results of triaxial tests on kaolin-sand mixtures with theoretical homogenization-based calculations, and also finite element analysis results (via CRISP program) on a simple model of a spherical particle at the center of a clay cube in triaxial loading condition. They observed that the sudden transition of response (in curves of stress ratio q/p' versus distortional strain) due to increase of grain contents above 45% in experiments, was falsely modeled as a gradual transition in theoretical and finite element analysis. Such unreal result might have been due to the false role that homogenization assumptions (and the simple finite element geometry analyzed by the code) gave to the grains, while they were (in low fractions) practically only ineffective fillers.

According to the latter concerns, in the current study only finite element analysis is performed on sample geometries almost similar to the real ones used in the experiments, and homogenization-based analysis was not applied. Such numerical analyses, performed on a thorough geometry model of a mixture of inclusions and finer material, has some precedent in the literature which has leaded to satisfactory results [e. g. 13, 14 and 15].

3. Experimental investigation

Heterogeneity of the mixtures response is mainly devoted to the local variation of matrix soil properties among inclusions. Such heterogeneity includes EPWP also, which however, is expected to tend to uniformity by time, due to redistribution of pressure. The rate of this uniformity formation depends on the permeability of the soil. To probe such trend of behavior, a wide range of permeability (from sand to compacted clay) were tested. Sand and silt materials were tested by torsional hollow cylinder apparatus, but the compacted clay was tested in cyclic triaxial apparatus, due to some difficulties with saturation of relatively large hollow specimens of clay. The largest possible specimen dimensions were preferred for this study to minimize effect of inner pressure transducers on behavior of the specimen. The 40 mm thick hollow cylinder specimens contained two inner transducers with 6 mm width. Satisfying ASTM standard [16] for largest inclusion size inside a triaxial specimen, 70 mm diameter for triaxial specimens was also selected, which contained one inner pressure transducer with 10 mm width.

3.1. Hollow cylinder testing equipment and procedure

A high capacity medium-sized hollow cylinder apparatus with capability of testing specimens up to 200 mm in outer diameter, 120 mm in inner diameter and 300 mm in height was used [17,18]. Outer and inner cell pressure were always the same, as the inner and outer spaces were connected, to decrease non-uniformity of stress and strain distribution throughout the hollow specimen.

To capture probable difference of near-field and far-field behavior, two inner miniature pressure transducers (IPT) were installed inside the specimen, one surrounded by inclusions resembling near-field situation, and the other floating in pure matrix relatively far from the inclusions (Fig. 2a). The aluminum cages of the IPTs (Fig. 2b) were solid enough to let the probable local densifications occur between inclusions and the transducer.

The inclusions were placed in a distance similar to those of a mixture with 40% volumetric concentration of the grains. In addition to the considerations taken into account from the literature to select such a distance, closer position of the inclusions was not desirable however, due to probable unsuccessful compaction of the matrix soils among the inclusions and the transducer.

A high capacity differential pressure transducer (HCDPT) measured difference of cell pressure and average of pore water pressure at top and bottom of the specimens. As cell pressure was separately measured by an external pressure gauge, average of pore water pressure at top and bottom of the specimen could be evaluated based on HCDPT results.

To saturate the specimens, the so called double-vacuum method [19] was employed, in which complete vacuum (-98 kPa) was applied to the specimen as back pressure, while keeping the initial effective stress constant by applying a partial vacuum of required magnitude to the cell. Then the de-aired distilled water prepared in advance was allowed slowly to enter from the bottom of the specimen replacing the air in voids. Expelled air was taken out from the top of the specimen into a drainage tank, while the complete vacuum

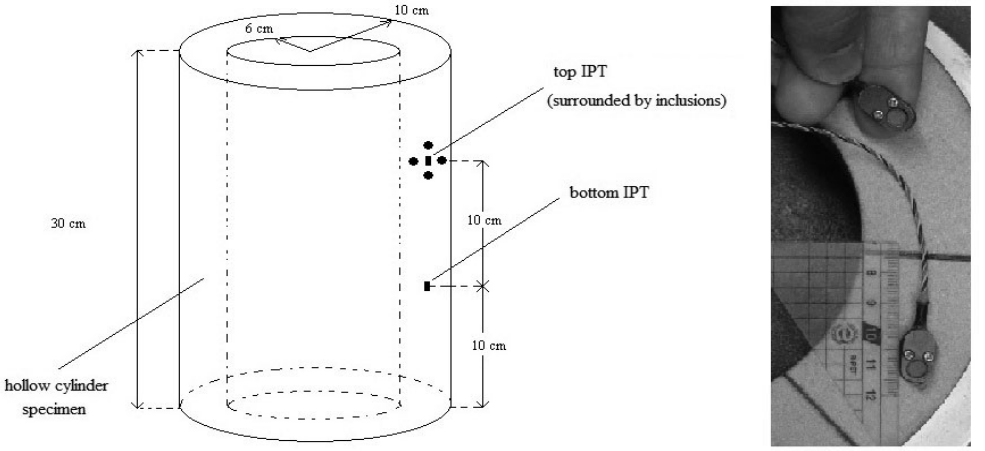

Fig. 2. a) Schematic of inner pressure-transducers (IPT) positions inside the hollow cylinder specimen; b) Aluminum-cages containing miniature pressure transducers

was being applied to both distilled water tank and drainage water tank.

Considering different kinds of composite soils found in nature, a wide range of matrix materials were considered to be tested , and ceramic beads (G_s = 3.620) with a diameter of 5 mm (which was the maximum possible dimension of the inclusions according to specimen thickness) were used as inclusions. Results of such experiments would also be relevant to previous researches on composite-clays however; if a kind of difference of behavior could be detected between near- and far-field matrix of sand (D50 = 0.162 mm) or silt (finer than No.200 sieve) specimens, then it could be concluded that a higher contrast would occur in the clay material due to its higher plasticity.

3.1.1. Sand specimens

Sand (G_s=2.656, e_{min} = 0.632, e_{max}=0.992) specimens were prepared by air pluviation, and the initial relative density (D_r) of the specimens was controlled by falling height of sand grains through the funnel. The specimens (initial D_r around 50-53%) contained pure sand, and only few ceramic beads as inclusions around the top IPT, as schematically illustrated in Fig. 2a, and also shown in Fig. 3a.

The specimens were saturated (B≥98%), consolidated to 100 kPa pressure and subjected to 50 undrained cycles of shear strain with single amplitude (γ_{SA}) of 0.075% at a frequency of 0.1 Hz. The frequency was chosen near to previous studies range i.e. 0.005 and 0.01 Hz [1], and 0.1 Hz [7, 20], to have possibility of comparison of the trend of behavior with previous findings. After the first series of cycles, drainage valves were opened and the specimens were subjected to 300 kPa consolidation pressure and another similar sequence of undrained cycles were applied to them again. No difference was captured in EPWP generation between the IPTs, and also with average value at both ends of the specimens, in neither of the cyclic loadings.

A sand specimen was mixed thoroughly with ceramic beads also, and a mixture of 40% (volumetric) grain and 60% sand was attained (Fig. 3b), to see if any heterogeneous filed of pore water pressure could be captured throughout the specimen.

Based on the concept of effective void ratio which considers only the effective fraction of the mixture to determine its void

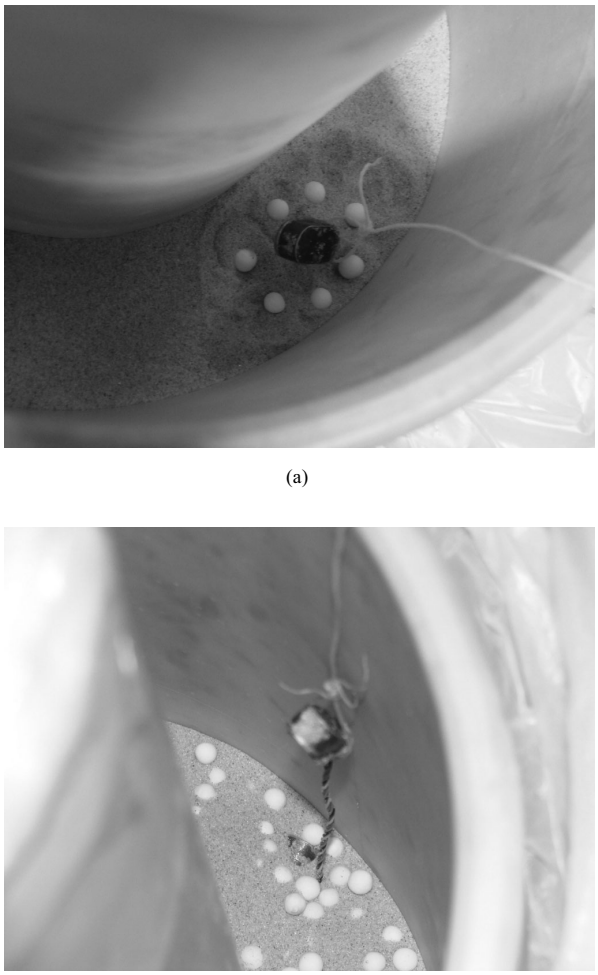

Fig. 3. a) Sand specimen with ceramic-surrounded top IPT; b) mixture of sand and ceramic with 40% volumetric granular content

ratio [21, 22, 23], and assuming that ceramic beads are floating in sand matrix, the minimum initial Dr of the mixture was evaluated as 66%. However, the real initial Dr of the sand fraction must have been higher, due to the voids that was captured between ceramic beads. Loading condition of this specimen was the same as previous ones, and also the results. No heterogeneity was captured at all. A typical result of eight tests on sand specimens is shown in Fig. 4, representing residual EPWP normalized to the initial effective confining pressure (U_r) in different cycles.

3.1.2. Silt specimens

Next step was examining silt (G_s = 2.665) specimens to see if any evidence of heterogeneity could be observed.

To compact the specimen up to a density nearly equal to 95% of the maximum dry

density of the material (which was equal to 15.3 kN/m^3 according to ASTM D698

procedure) at a water content 2% wet of optimum (w_{opt} = 21%), a ring-shaped hammer was designed which fitted the specimen dimensions well (Fig. 5a). As shown

in Fig. 5b, a hollow steel pipe around which hammer could move up and down was designed to protect IPTs during compaction. After completing each layer compaction, the areas around IPTs were compacted by the aid of a narrow steel bar, up to a density consistent with other areas of the specimen (Fig. 5b).

To achieve a uniform density all around the specimen height, two trial specimen were compacted and a trend similar to under compaction method [25] was chosen to avoid formation of denser bottom layers compared with top ones. The compaction was performed in 15 layers of 2 cm compacted thickness. Before placing the material of the next layer, the surface of the compacted layer was thoroughly scarified to a proper depth to ensure interlock between successive layers.

Position of top IPT and surrounding grains are shown in Fig. 5b. Loading procedure was also exactly the same as those applied on sand specimens.

Again no difference was observed in the pore pressure generated throughout the specimens. Fig. 6 shows a typical result of six tests on silt specimens.

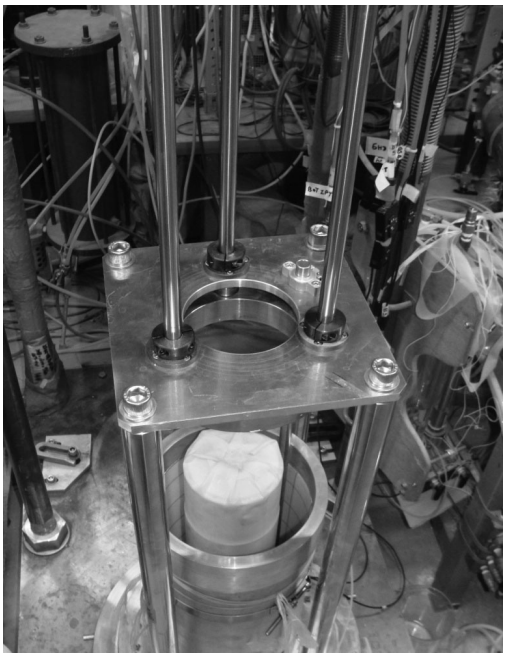

(a)

(b)

Fig. 5. a) Ring-shaped hammer for compaction of the specimen; b) hollow steel pipe to protect IPTs during compaction, top IPT position and surrounding grains in silt specimens

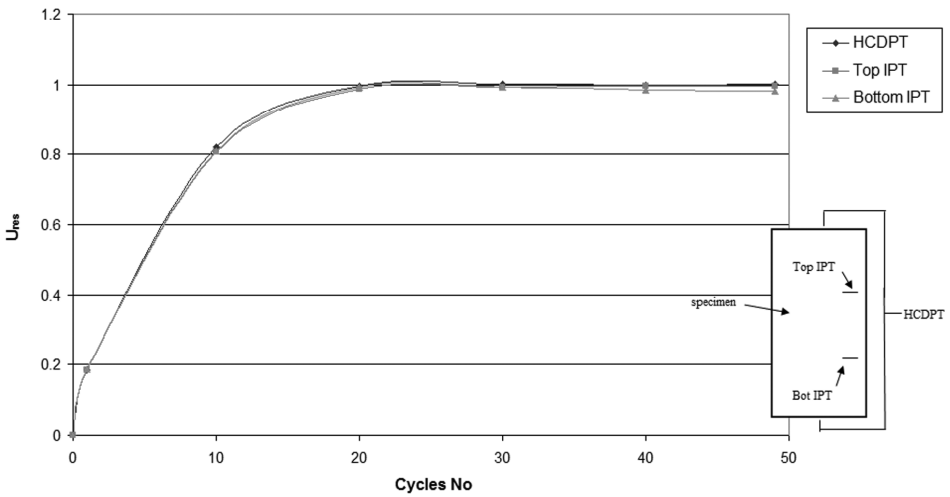

Fig. 4. Typical change of excess pore water pressure with time at both ends and also inside the sand specimens during cycles of loading

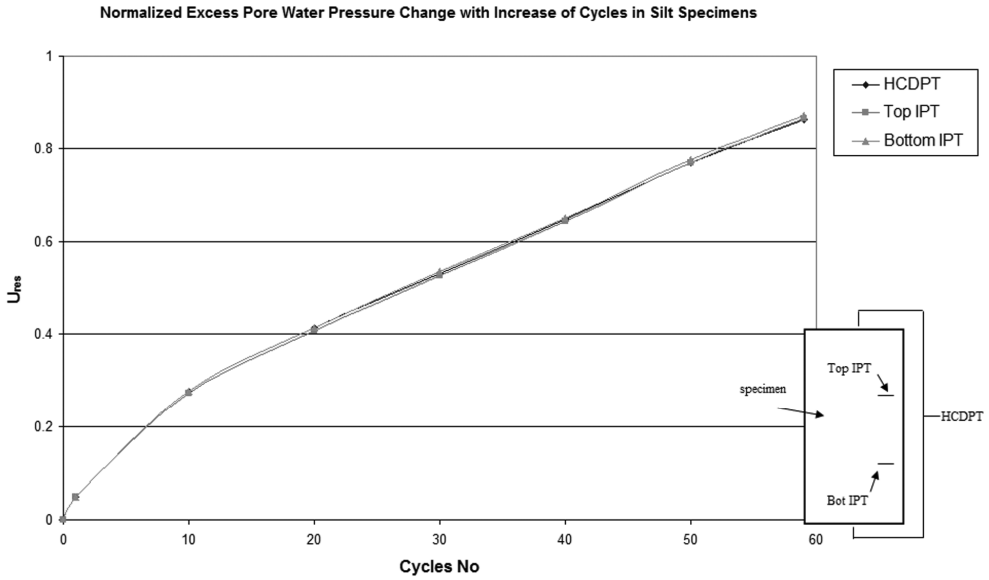

Fig. 6. Typical change of excess pore water pressure with time at both ends and also inside the silt specimens during cycles of loading

3.1.3. clay specimens

In initial tests on clay material, inclusions were not placed in the specimen and EPWP distribution was examined throughout the pure specimens. To achieve a more uniform compacted layer for clay material (G_s = 2.731), a small tamper was replaced with the ring shaped hammer, which is shown in Fig. 7. To have a uniform density at top and bottom of each layer by using the relatively small tamper, compaction was performed in 20 layers of 1.5 cm compacted thickness.

First two specimens which were compacted by the tamper, achieved 95% of the standard maximum dry density of the clay material, 2% wet of optimum (γ_{drymax} =14.5 kN/m^3, w_{opt} = 26.5%). However, due to the small size of the tamper, bottom of each layer was not well compacted, leading to initially heterogeneous specimens.

To avoid such weakly compacted specimens, compaction effort was increased in next series of experiments, leading to a dry density equal to 100% of the standard maximum dry density of the material. However, due to the relatively large dimensions of the specimen, it was very difficult to saturate the clay (LL=44.5%, PI=13.5%) specimens properly in reasonable time duration. Though 48 hours were given to each specimen to soak de-aired water, the B-value after application of 200 kPa back pressure was equal to 90% which was not satisfactory at all. Giving more time to each specimen to saturate was not a practical solution due to the cell-water air conduction into the specimen during long period of saturation and consolidation which would take more than a week. Increase of back pressure was not also possible due to the 500 kPa capacity of IPTs, considering 300 kPa effective confining pressure. Reduction of the specimen size was not also preferred due to the size of inner transducers.

Results of 2 tests on these densely compacted specimens are shown in Fig. 8a (γ_{SA} = 0.4%, f = 0.05 Hz) and Fig. 8b (γ_{SA}= 0.75%, f = 0.03 Hz). Maximum torsional speed of the apparatus was utilized in these two tests. As obvious in these figures, IPTs measured a magnitude up to 20% different with the average of values at both ends of the specimens.

It is also worth noting that despite the case in silt specimens (γ_{SA} = 0.075%, f = 0.1 Hz ; Fig. 9a), in clay specimens the amplitude of EPWP fluctuation is different in different locations of the specimens, as shown in Fig. 9b and 9.c. In this figure, U_{max} and U_{min} are the maximum and the minimum EPWP at the cycle respectively, normalized by initial effective confining pressure. As obvious in this figure, increase of strain amplitude from 0.4% to 0.75% in clay specimens, increased the difference between top & bottom IPTs amplitudes, though frequency of loading was decreased from 0.05 Hz to 0.03Hz (Fig. 9b and 9.c).

As a consequence of the specimen saturation problem, test on clay materials having inclusions inside were not conducted in Japan. Triaxial specimens with 70 mm diameter and 140 mm height were preferred to hollow cylinder ones, and tests were continued in Iran.

Fig. 7. Tamper used for compaction of clay specimens

3.2. Cyclic triaxial testing equipment and procedure

Cyclic triaxial tests were performed at IIEES geotechnical laboratory. Only one IPT was placed at the middle elevation of the specimen (Fig. 10). Pore water pressure was captured at three points, i.e. top, middle (by IPT) and bottom of the specimen. The IPT had the capacity of 1000 kPa pore water pressure measurement.

Two types of specimen, i.e. pure clay (LL = 32, PI=12) and mixture of clay with ceramic beads (D= 4 mm, G_s = 3.73) were prepared and tested (Fig. 10). Pure clayey specimen (10a) only contained the IPT at the middle part. Totally mixed specimens contained 40% (volumetric) ceramic beads with 4 mm diameter and 60% clay, again with the IPT at the middle part (Fig 10b).

The specimens were compacted in 10 layers to the 95% of maximum dry density of the material (which was equal to 17.2 kN/m^3 for pure clay and 23 kN/m^3 for mixed material, according to ASTM D698 procedure) at a water content 2% wet of optimum (w_{opt} = 16% for pure clay, and 8.1% for the mixed one). Before placing the material of the next layer, the surface of the compacted layer was scarified to ensure interlock between successive layers. Similar to silt specimens, trial specimens were compacted and a trend similar to under compaction method [25] was chosen to avoid formation of denser bottom layers compared with top ones, especially for pure specimens. Anti-frictions were utilized at both ends to facilitate a more uniform deformation pattern of the specimen all along its height.

To saturate the specimen, CO_2 circulation was followed by circulation of de-aired water through the specimen, and then 400 kPa backpressure was exerted on the specimen, waiting (up to 3 or 4 days) to reach a B value not less than 95% at top, middle (measured by the aid of IPT) and bottom of the specimen.

The specimen was then consolidated to 300 kPa effective confining stress isotropically, and subjected to 50 undrained

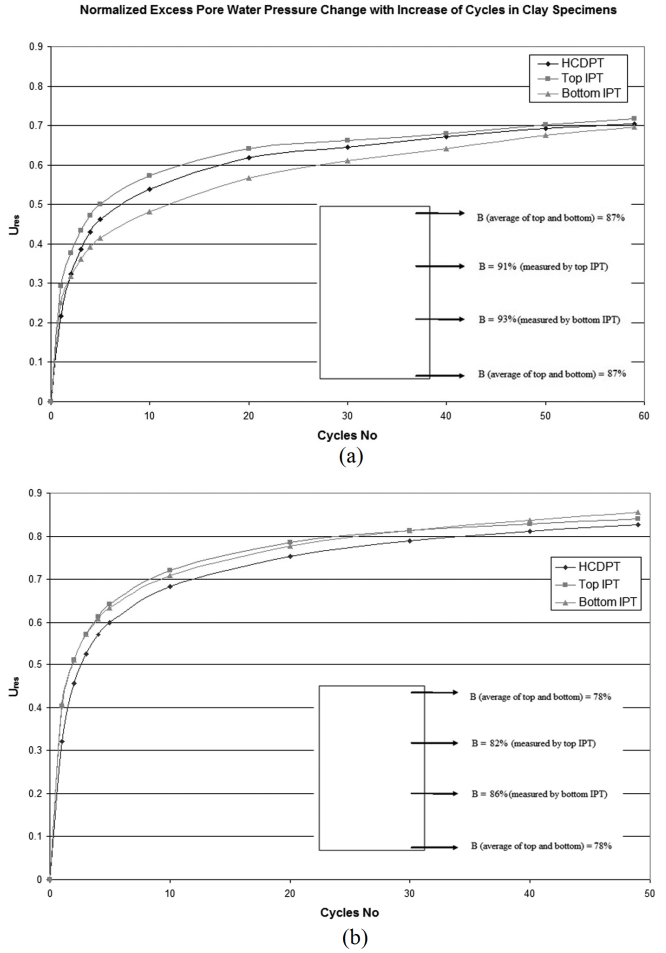

Fig. 8. Change of excess pore water pressure with time at both ends and also inside the clay specimen during cycles of loading: a)γSA= 0.4%, f = 0.05 Hz; b) γSA = 0.75%, f = 0.03 Hz

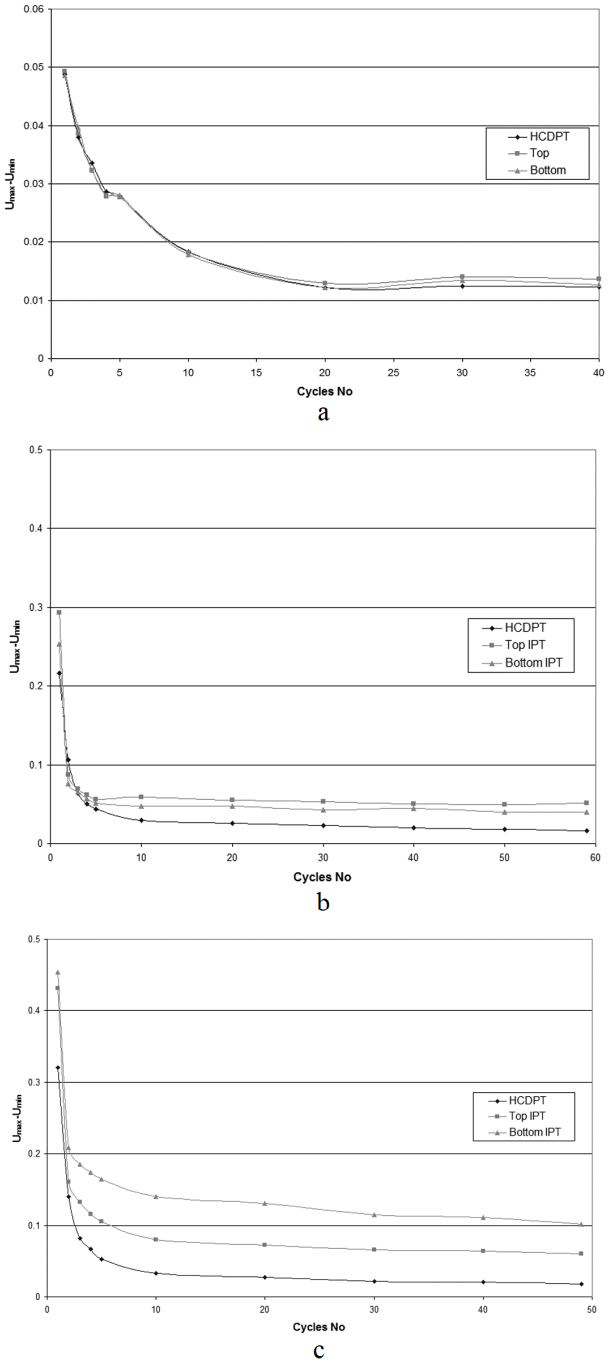

Fig. 9. Amplitude of excess pore water pressure change at both ends and also inside the: a) silt specimen (γ_{SA} = 0.075%, f = 0.1 Hz); and clay specimens with: b)γ_{SA}= 0.4%, f = 0.05 Hz; c) γ_{SA} = 0.75%, f = 0.03 Hz loadings

(a)

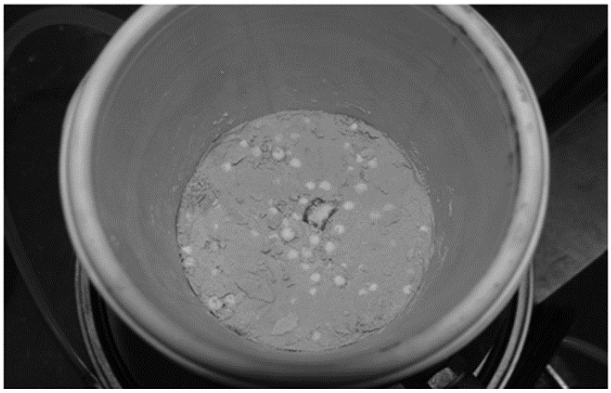

(b)

Fig. 10. Clay specimens for cyclic triaxial test: a) pure clay specimen; b) mixed specimens

cycles of shear strain with single amplitude of 1% at a frequency of 0.1 Hz.

Fig.11a to 11c show results of the tests at top, middle and bottom of pure and mixed specimens respectively. Though difficult to find a trend, it is observed in the figure that the expected increase of residual excess pore pressure by increase of grain content, which was a prominent feature of previous studies [1, 7] is not clearly observed herein. Totally 12 tests were conducted with this frequency to be sure of the repeatability of the behavior.

As probable heterogeneity seemed to have enough time to redistribute in this frequency of loading, and to probe role of frequency in formation of heterogeneity, the test on pure and totally mixed specimens were repeated with frequencies of 0.01 Hz and 1 Hz, results of which are shown in Fig. 12 and 13 respectively.

As obvious in these figures, results of different frequencies of loading follow the same tendency, in terms of residual excess pore pressure accumulation by increase of cycles, as previous experiments with 0.1 Hz frequency of loading: the expected increase of EPWP by increase of inclusions is not observed. However, by increase of frequency of loading, amplitude of EPWP cycles decrease at the middle part, as shown in Fig. 14. As evident in this figure, the trend of decrease of amplitude at the middle of specimens is not captured at top and bottom, which shows increase of non-uniformity of stress and strain distribution by increase of frequency of loading.

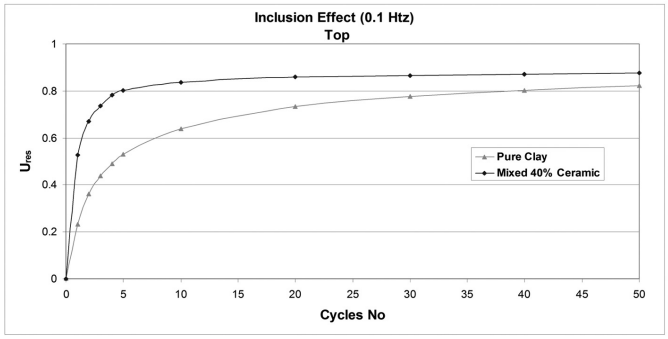

(a)

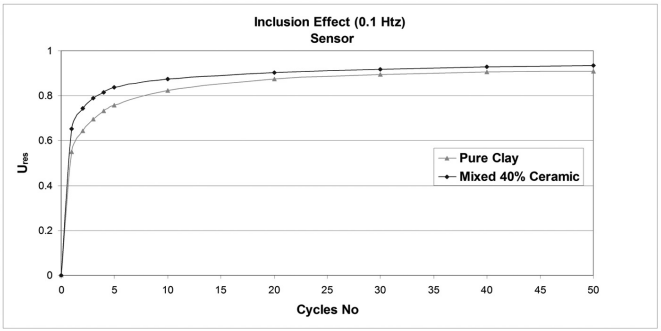

(b)

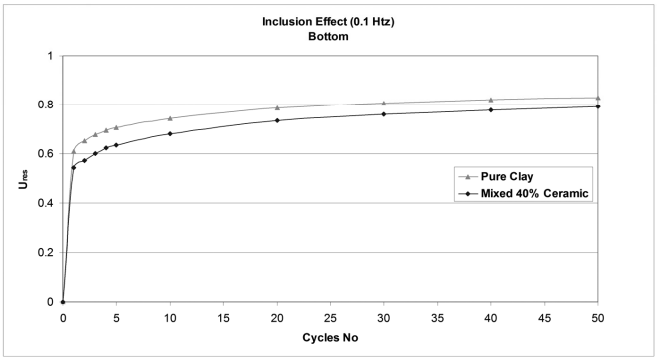

(c)

Fig. 11. Normalized residual excess pore water pressure change with increase of cycles at frequency of 0. 1 Hz at a) top; b) middle; c) bottom of the specimens

3.3. Discussion on experimental results

The similar trend of uniform EPWP distribution along the sand, silt and low-plastic clay specimens with or withought inclusions, during undrained cyclic loadings (at equal or higher frequency of loading in comparison with those reviewed in the literature [1, 7, 16]) maybe mainly devoted to substantial hydraulic conductivity of the materials used as the matrix, compared with fat clay ones which showed non-uniform results as stated in the literature. Any probable local increase of pressure in such relatively permeable materials is redistributed quickly throughout the specimen.

Increase of confining pressure could also help formation of heterogeneity. However, as the capacity of inner transducers utilized in the current study was 500 kPa for silt specimens in hollow cylinder, and the capacity of cell pressure was 700 kPa in triaxial cell, it was not possible to increase effective confining pressure over 300 kPa, considering initial 200 kPa and 400 kPa backpressures utilized to saturate silt and clay

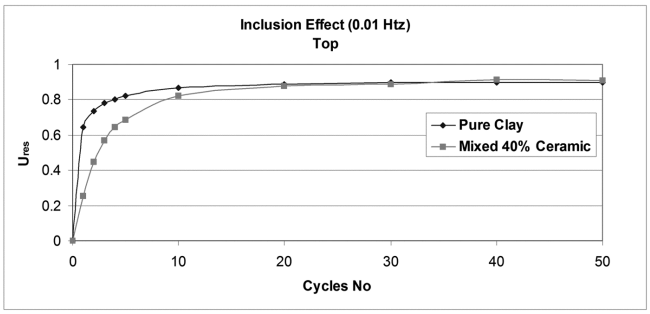

(a)

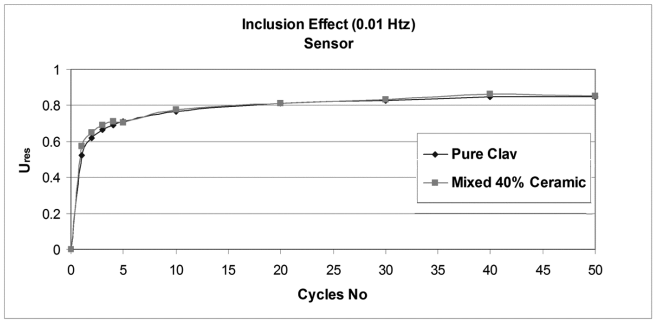

(b)

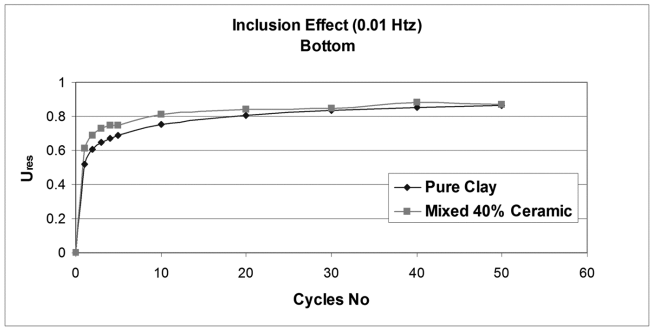

(c)

Fig. 12. Normalized residual excess pore water pressure change with increase of cycles at frequency of 0. 01 Hz at a) top; b) middle; c) bottom of the specimens

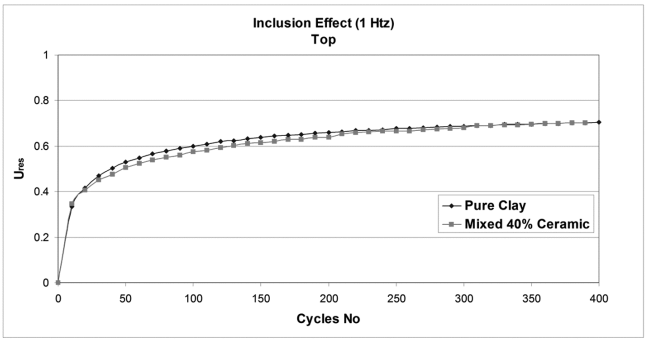

(a)

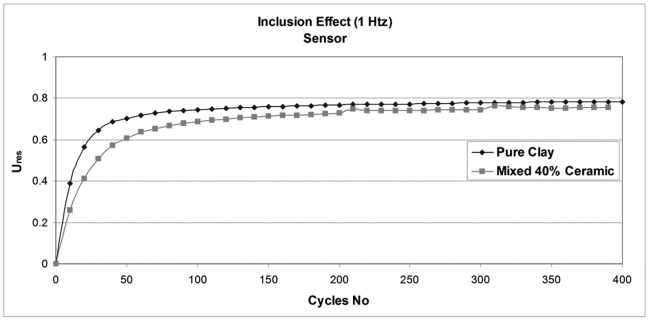

(b)

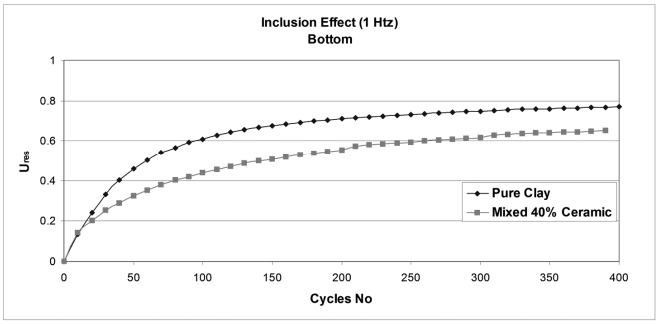

(c)

Fig. 13. Normalized residual excess pore water pressure change with increase of cycles at frequency of 1 Hz at a) top; b) middle; c) bottom of the specimens

specimens respectively.

Using materials of higher plasticity and lower permeability also seemed impossible, because saturation of the relatively large specimens (dimensions of which were forced due to inner sensor size) could hardly be achieved by the limited confining cell pressure (and consequently back pressure) available at the laboratory.

It is possible to highlight heterogeneity of excess pore pressure by increase of loading rate. However, it will cause non-uniformity of pore pressure generation throughout pure specimens, and consequently no clear trend may be detected comparing mixed and pure specimens in high rates of loading, as experienced in this study.

It seems that with the current miniature sensor utilized at this study (which is also used at geotechnical laboratories of university of Tokyo for measuring pore pressure inside sand specimens), and consequent relatively large specimen dimensions, it is not possible to probe a clear trend in mixed-clay specimens. Both the sensor and specimens should be smaller to assist meaningful tests in clayey materials while capturing pore pressure in numerous locations inside the specimen, which requires high tech and costly instruments.

4. Numerical investigation

For a better understanding of the mixed-clay behavior, parallel to experimental investigation, numerical investigation on triaxial specimens of clay also was carried out continuously, results of which assisted better understanding of the observed behavior during experiments. It is evident that by the aid of numerical analysis, it is possible to capture (in detail) the EPWP, as well as stress and strain distribution throughout the specimen, despite the experimental results in which only EPWP changes were surveyed in limited locations.

Numerical analyses were performed via Plaxis 3D (version 2010.02) and 2D (version 2010) finite element code [26, 27]. 3D analyses were performed on dry specimens while for saturated specimens the 2D code was used to avoid time consuming 3D undrained calculations. Dry analyses were conducted to explore effect of inclusions on stress and strain

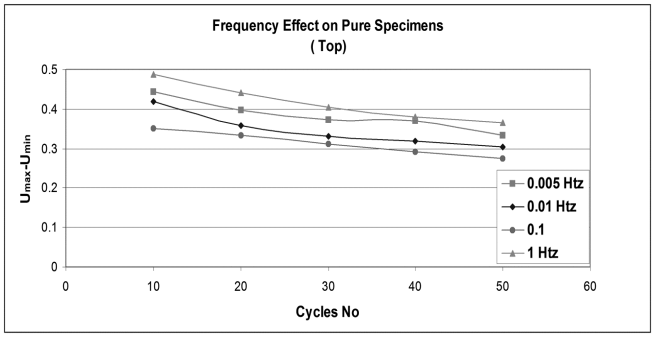

(a)

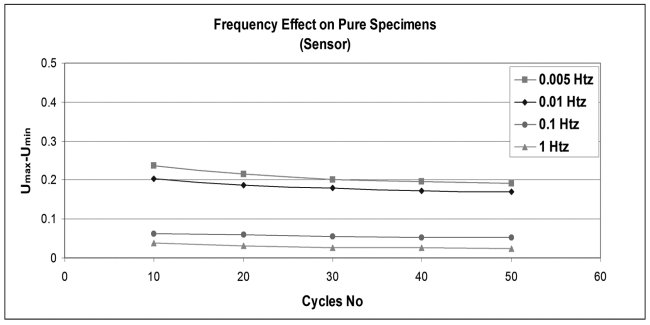

(b)

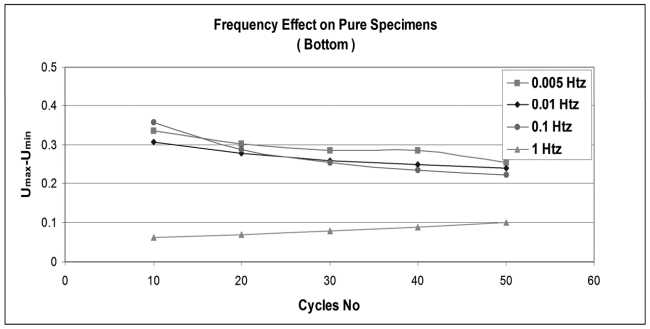

(c)

Fig. 14. Effect of frequency of loading on excess pore water pressure fluctuation during loading cycles at a) top; b) middle; c) bottom of the specimens

distribution throughout the specimen, and saturated specimens were also modeled to probe pore water pressure heterogeneity and its redistribution trend with time.

The dimensions of the specimen and also the inclusions diameter were the same as those of real ones in the experiments. However, only few inclusions were modeled to avoid complexity of the geometry and concentrate on qualitative behavior of the inclusions effect on heterogeneity of stress and strain distribution throughout the specimen. In 2D analysis, the inclusions were located only in the axis of symmetry in a nearly half-circular shape to resemble a sphere (Fig. 16 and 21).

To model anti-frictions used in experiments at both ends of the specimens, an interface was modeled at the bottom of the geometry in 3D model, to let the specimen expand horizontally while loaded in vertical direction. Top of the geometry had no fixities and could have the same deformation pattern as the bottom. In 2D model however, the bottom was free to move horizontally, except the point on

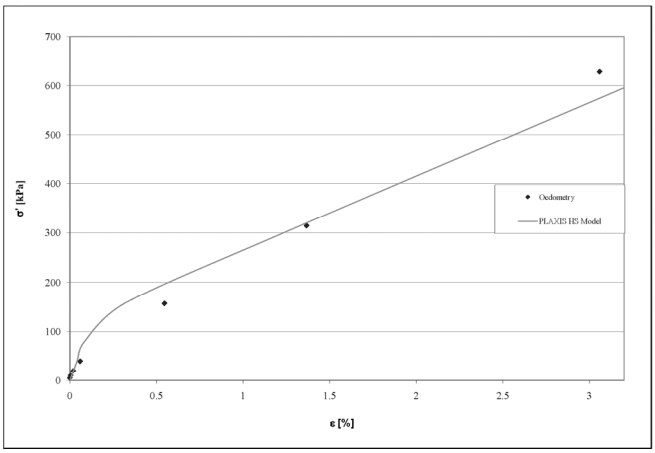

Fig. 15. Vertical stress versus vertical strain from Oedometry test and those simulated in Plaxis by Hardening Soil model

symmetry axis.

Hardening-Soil material model of the code was preferred for the matrix soil, which is based on hyperbolic model, benefiting also from isotropic hardening both in shearing and compression loadings [28]. Inclusions were also modeled as linear-elastic solid materials, with a shear modulus nearly one thousand times of that of the matrix in average strain magnitudes, to resemble solid granules behavior in real clay-aggregate mixtures. The geometry of the inclusions was modeled by spheres of 9 mm diameter.

To calibrate material model parameters, a series of Oedometer tests were performed on the clay material. Fig. 15 shows the Oedometr test results and those calculated in the code in similar loading condition. Table 1 shows the calibrated parameters of the material model employed in this study for both 3D and 2D analyses.

Vertical strain was applied monotonically, because the utilized isotropic-hardening material model is not capable of capturing accumulation of plastic volumetric strains during sequences of unload-reload, which is the prominent feature of soil behavior during cyclic loadings (kinematic hardening). However, the results are meaningful from a qualitative point of view.

Table 1. Calibrated parameters of Hardening-Soil material model applied in numerical analysis

Parameter	Name	Unit	Clay
Dry unit weight	γ_{unsat}	kN/m^3	18
Saturated unit weight	γ_{sat}	kN/m^3	19.1
Horizontal permeability	k_x	m/s	1.E-9
Vertical permeability	k_y	m/s	1E-9
Secant stiffness (shear hardening)	E^{ref}_{50}	kN/m^2	15000
Tangent oedometer stiffness (compression hardening)	E^{ref}_{oed}	kN/m^2	15000
Unloading-reloading stiffness	E^{ref}_{ur}	kN/m^2	60000
Power for stress dependant stiffness (hyperbolic model)	m	-	0.15
Reference stress (hyperbolic model)	P_{ref}	kN/m^2	600
Cohesion (perfect plasticity limit)	c	kN/m^2	40
Friction angle (perfect plasticity limit)	ϕ	°	35
Dilatancy angle	ψ	°	0

4.1. Analyses on dry specimens

During dry analyses confining stress was kept equal to 300 kPa, and a magnitude of vertical load was chosen similar to the single amplitude of loading cycles in the experiments, i.e. 1% vertical strain, was exerted on the specimen. It seemed reasonable to seek the heterogeneity formation in such loading patterns, as the reported precedent of heterogeneous stress distribution throughout specimens of mixed soils in the literature were also based on results of both monotonic and cyclic triaxial loadings [1].

Inclusions were located in two different patterns: aligned vertically with axial loading direction (Fig. 16a) and aligned horizontally perpendicular to axial loading direction (Fig 16b).

Fig. 17 and 18 show typical patterns of volumetric strain distribution after loading, in the sections of the specimen where inclusions are located. As evident in these figures, two different patterns of behavior are observed: when inclusions are located vertically aligned, i.e. in the direction of axial loading, there is a concentration of strain through the soil captured between the inclusions; but when inclusions are located horizontally, there is a reduction of strain concentration in the soil, from the average magnitude of strain in other inclusion-free levels of the specimen. The combination of these situations would lead to a stress and strain distribution, totally dependent on the inclusions distance and position relative to loading direction (Fig. 19). Mean stress ($p = (\sigma_1+\sigma_2+\sigma_3)/3$) distribution also follows the same tendency as that of volumetric strain, as shown in Fig. 20.

Based on extensive numerical analyses with different number of inclusions and different patterns of inclusion distribution and loading direction, it may be qualitatively concluded that inclusions form a heterogeneous filed of stress and strain throughout the surrounding matrix. Consequently increase, decrease or no change of stress and strain magnitudes from the expected average inside inclusion-free matrix soil may occur. In areas between inclusions where negative deviatoric stress ($sij=\sigma_{ij}-\delta_{ij}<0$)

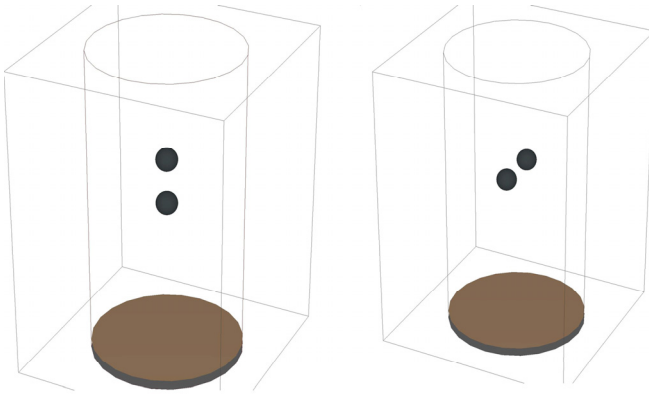

Fig. 16. Position of inclusions during analysis: (a) vertically aligned; (b) horizontally aligned

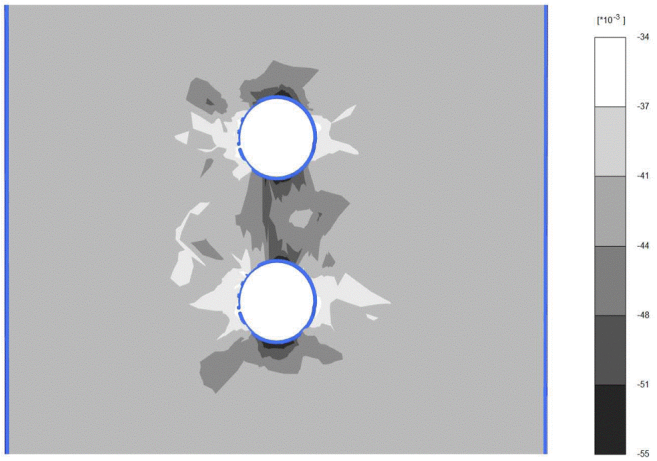

Fig. 17. Volumetric strain distribution in a section of the triaxial specimen containing vertically aligned inclusions

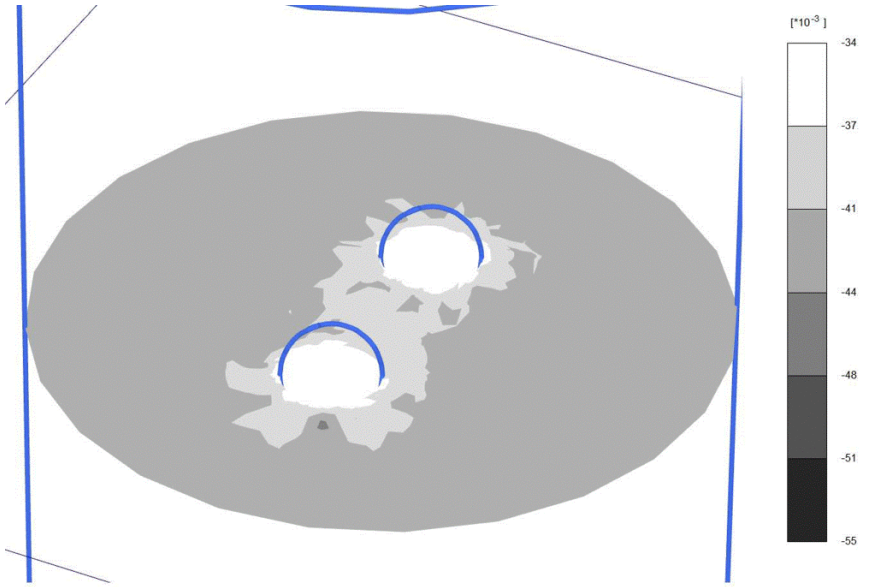

Fig. 18. Volumetric strain distribution in a section of the triaxial specimen containing horizontally aligned inclusions

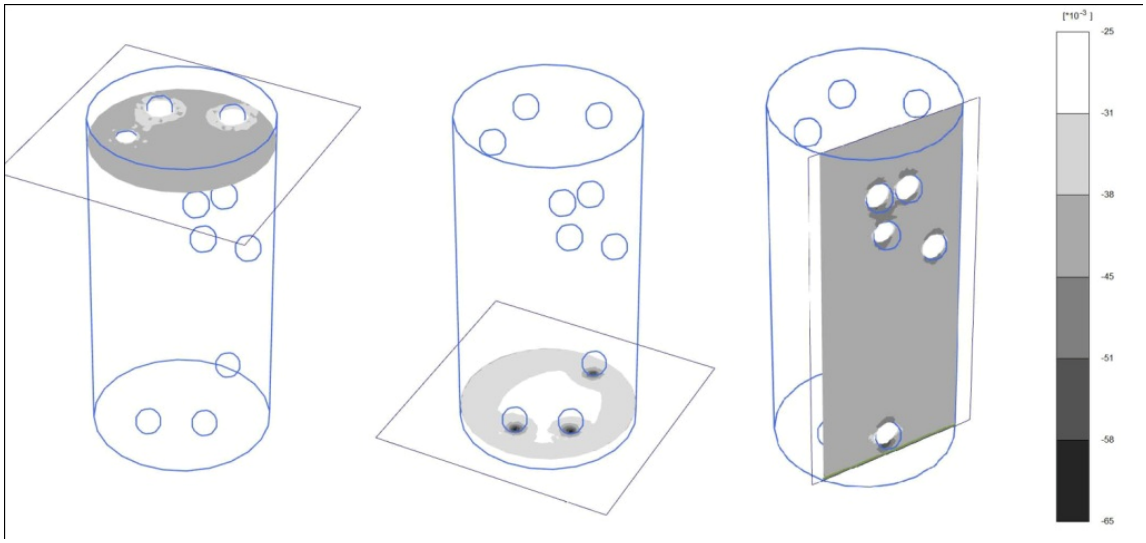

Fig. 19. Volumetric strain distribution in three different sections of a triaxial specimen containing randomly aligned inclusions

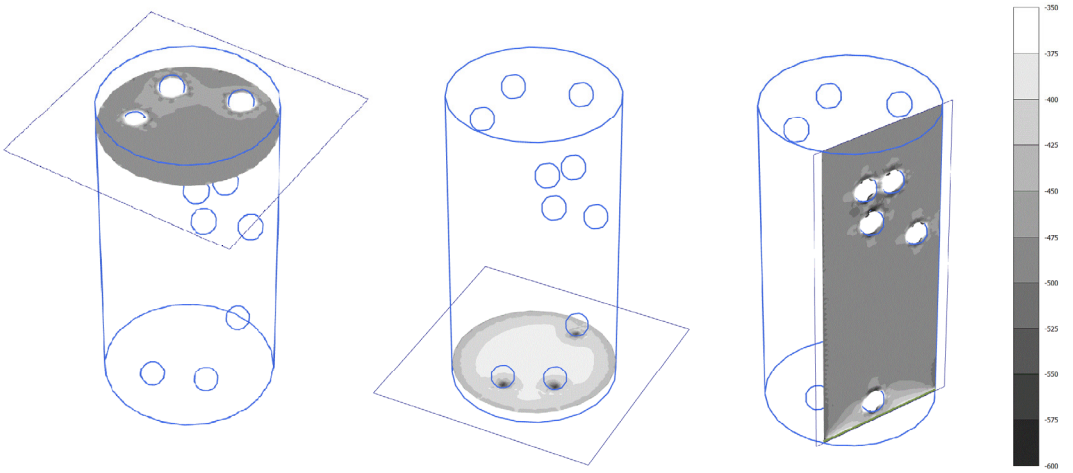

Fig. 20. Mean stress distribution in three different sections of a triaxial specimen containing randomly aligned inclusions [kPa]

is induced, lower magnitudes of volumetric strain and mean stress, compared with the expected magnitude in pure specimens, are produced; while in areas of positive deviatoric stress, higher volumetric strain and mean stress are produced. The term "extension path" and "compression path" will be used to describe the trend, respectively.

4.2. Analyses on saturated specimens

After some experiences of undrained analyses in 3D code, which were too time consuming and also unstable in calculation with the complex sphere geometries of inclusions, 2D code was preferred for saturated specimens. To ensure reliable results, similar geometry of 3 vertical inclusions located at the center of the dry specimen were modeled in both 2D (Axisymmetric) and 3D code (Fig. 21) and volumetric strain after a 300 kPa confining pressure and 1% axial strain was compared, as shown in Fig. 22. As evident, the trend of behavior is the same, only differing slightly in magnitude, which is mainly due to accuracy of inclusion geometry in 2D code.

In undrained analysis, with the previously mentioned loading situation, the heterogeneity of EPWP is formed, as a consequence of the non-uniform stress and strain distribution. However, based on the permeability of the matrix material, the pore pressure redistribution would lead to a uniform state throughout the specimen. Fig. 23 to 26 show such trend of behavior clearly. After consolidating the specimen to 300 kPa confining pressure, 1% vertical strain was exerted on the material in undrained condition instantly, and then time was given to the material for EPWP redistribution (with all boundaries close to flow in or out). After nearly 1.5 seconds, the pressure was uniformed thoroughly, though at the beginning 100% difference was observed in different areas of the soil (Fig 23). Fig. 25 and 26 show change of EPWP with axial strain and time respectively, from the beginning of axial straining in the mentioned undrained loading pattern, at three points which are located as shown in Fig. 24. It is also worth noting that the magnitude of strain among inclusions is greater

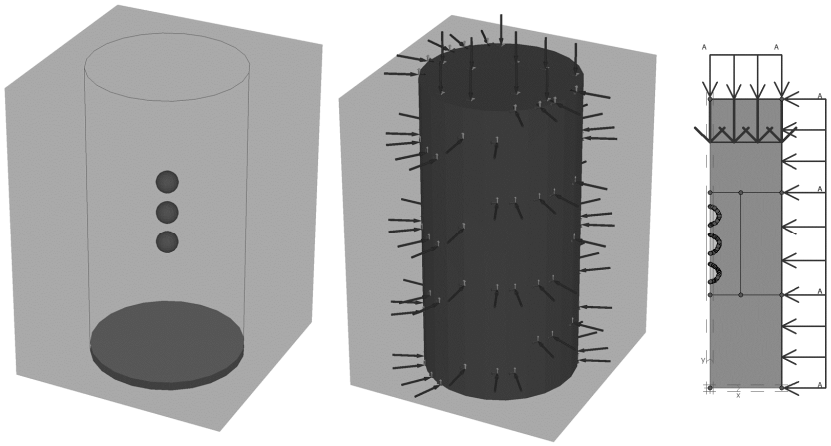

(a) (b) (c)

Fig. 21. Geometry of 3D and 2D axisymmetric model of triaxial specimen in finite element code

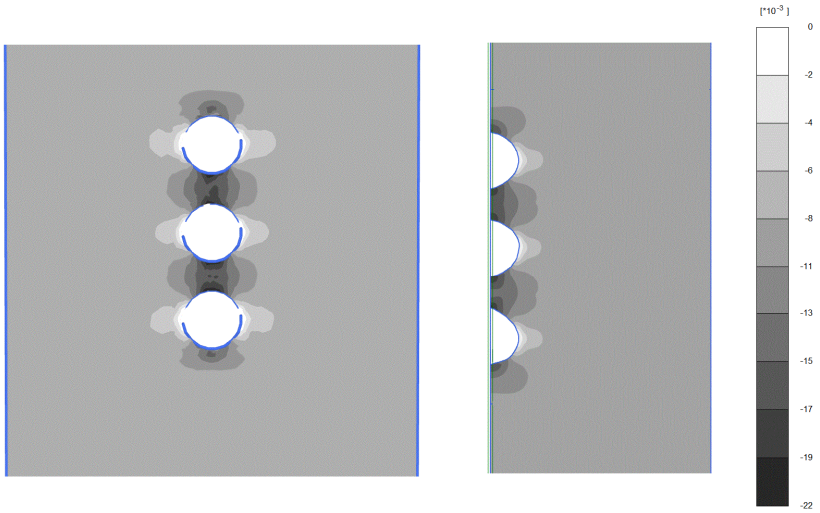

(a) (b)

Fig. 22. Volumetric strain distribution in middle section of the: a) 3D geometry of the triaxial specimen; b) 2D geometry of the triaxial specimen, containing vertically aligned inclusions

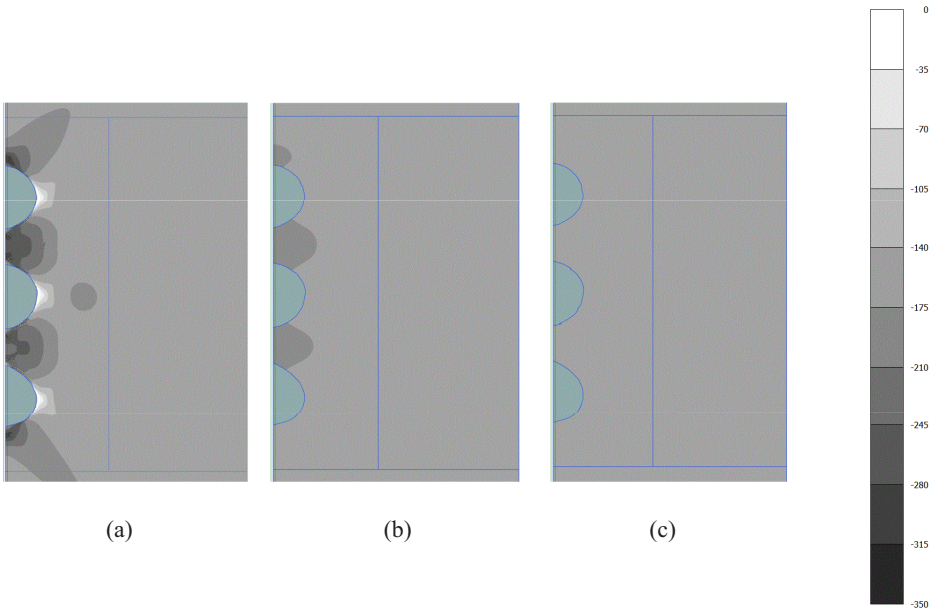

(a) (b) (c)

Fig. 23. Excess pore water pressure : a) instantly after loading; b) redistributed after 0.25 seconds; c) redistributed after 2.5 seconds in the middle part of a triaxial specimen geometry

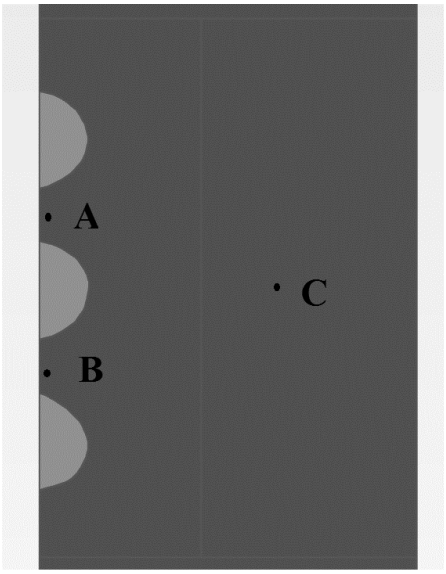

Fig. 24. Locations of three points where pore pressure change was captured during analyses

than areas far from inclusions, which is consistent with 3D analyses results.

To clarify role of permeability on rate of pore pressure redistribution, the analysis was repeated with a permeability 1/100 of the previous magnitude. As shown in Fig, 27, with decrease of permeability, time required to reach a uniform pore pressure throughout the specimen is increased from nearly 2 second to nearly 80 second, as expected.

However, this is mainly a qualitative observation of the trend; for a quantitative investigation of such local heterogeneities, more detailed analytical studies will be conducted by the authors.

5. Conclusion

A series of experimental and numerical investigations were conducted to observe formation of local heterogeneities of stress, excess pore water pressure and strain among inclusions, as a trend of behavior of composite soils. Concluding remarks are as follows:

1. Heterogeneity of stress and strain distribution in dry specimens was observed in numerical analyses results. Position of the inclusions relative to loading direction, and the distance between inclusions would lead to formation of "compression path" (positive deviatoric stress) and "extension path" (negative deviatoric stress) among inclusions. In "compression path" higher magnitudes of volumetric strain and mean stress were observed, compared with the magnitude in pure specimens, while in "extension path", lower magnitudes were observed.

2. Heterogeneous excess pore water pressure distribution in saturated specimens was formed during undrained numerical analyses. However, as qualitatively observed in these analyses, the heterogeneous excess pore water pressure induced among inclusions during loading, is redistributed with a rate proportional to material hydraulic conductivity.

3. In sand and silt specimens, any heterogeneity of pore pressure may hardly be captured, while in clay specimens, it may be possible to observe the heterogeneity in the tested

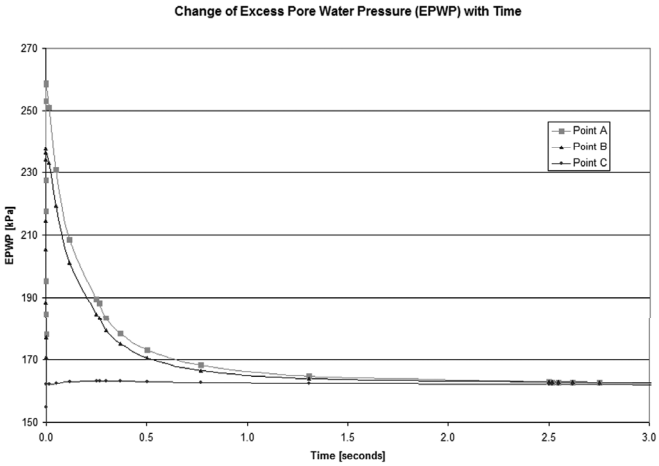

Fig. 26. Change of excess pore water pressure with time at three locations near and far from inclusions inside clay specimen (permeability = 3×10^{-9} m/s)

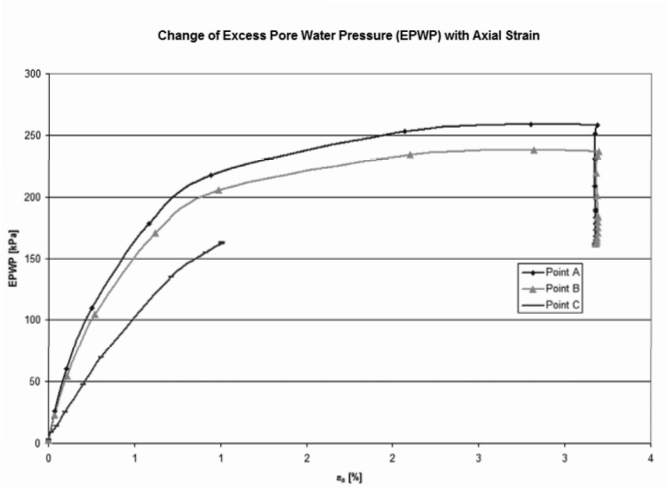

Fig. 25. Change of excess pore water pressure with axial strain at three locations near and far from inclusions inside clay specimen

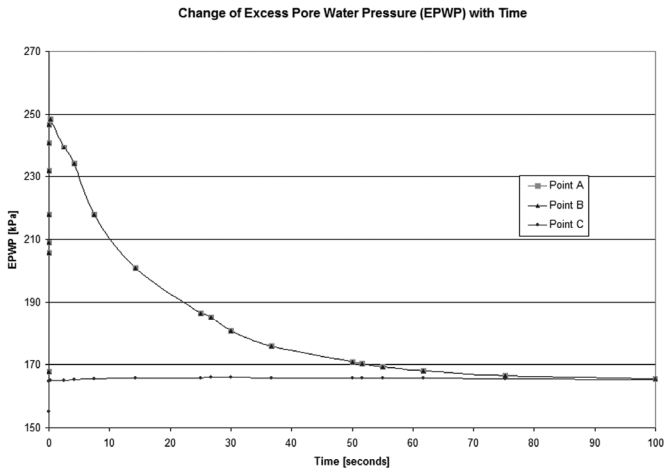

Fig. 27. Change of excess pore water pressure with time at three locations near and far from inclusions inside clay specimen (permeability = 3×10^{-11} m/s)

range of frequencies, depending on its plasticity and permeability.

It is however evident that change of excess pore pressure in any point of the mixed material depends on the initial consolidation stress, and subsequent loading stresses, which in some cases may even lead to reduction of excess pore water pressure.

4. With current available miniature sensors, which are currently used at geotechnical laboratories of university of Tokyo for measuring pore pressure inside sand specimens, it seems not possible to capture a clear trend of pore pressure distribution in mixed-clay specimens. Smaller sensors should be positioned in different parts of the relatively small specimens of the mixed material to achieve reliable results, which requires high tech and costly instruments.

Acknowledgements: This study was mainly supported by the International Institute of Earthquake Engineering and Seismology, Iran and also Industrial Institute of Science, The University of Tokyo, Japan, which are gratefully acknowledged. The authors also thank Dr. G. Chiaro and Dr. L. I. N. De Silva for their useful helps while doing the experiments in Japan, and also acknowledge Mr. M. Asgari, Mr. G. Hadavi and Mr. S. Azaadmanesh for their assistance in conducting the tests in Iran.

References

[1] Jafari, M. K. and Shafiee, A.: 2004, Mechanical behavior of compacted composite clays, Canadian Geotechnical Journal, 41(6): 1152-1167. doi:10.1139/T04-062.

[2] Fragaszy, R. J., Su, J., Siddiqi, F. H., Pedersen, H. A., Ho, C. L.: 1992, Characterization of heterogeneous soils using surface waves: Homogenization and numerical modeling, ASCE Journal of Geotechnical Engineering, 118(6): 920-935.

[3] Vallejo, L. E., Mawby, R.: 2000, Porosity influence on the shear strength of granular material clay mixtures, Engineering Geology, 58: 125-136.

[4] Kumar, G. V. and Muir Wood, D.: 1999, Fall cone and compression tests on clay-gravel mixtures, Geotechnique, 49(6): 727-739.

[5] Muir Wood, D., Kumar, G. V.: 2000, Experimental observations of behavior of heterogeneous soils, Mechanics of Cohesive-Frictional Materials, 5: 373-398.

[6] Jafari, M. K. and Shafiee, A.: 1998, Dynamic behavior of mixed materials used fore core of Karkhe dam, In proceeding of the 11th Europpean conference on earthquake engineering, Balkema, Rotterdam, The Netherlands, p. 179.

[7] Soroush, A. and Soltani-Jigheh, H.: 2009, Pre- and post-cyclic behavior of mixed clay soils, Canadian Geotechnical Journal, 46(2): 115-128. doi:10.1139/T08-109.

[8] Shafiee, A.: 2008, Permeability of compacted granule-clay mixtures, Engineering Geology, 97: 199-208.

[9] Gutierrez, M.: 2002, Discrete and homogenous modeling of geotechnical systems, an overview, In Proceedings of NSF workshop on Geotechnical Composite systems, Roanoke. pp. 28-31.

[10] Gutierrez, M.: 2003, Mixture theory characterization and modeling of soil mixtures, In Proceedings of the First Japan-U.S. Workshop on Testing, Modeling and Simulation, Geotechnical Special Publication, ASCE, 143: 600-616.

[11] Wang, J.G., Leung, C. F., Ichikawa, Y.: 2002, A simplified homogenization method for composite soils, Computers and Geotechnics, 29: 477-500.

12] Wickland, B.E., Wilson, G. W., Wijewickreme, D., Klein, B.: 2006, Design and evaluation of mixtures of mine waste rock and tailings, Canadian Geotechnical Journal, 43: 928-945. doi:10.1139/T06-058.

[13] Chammas, R., Abraham, O., Cote, P., Pedersen, H. A., Semblat, J. F.: 2003, Characterization of heterogeneous soils using surface waves: Homogenization and numerical modeling, International Journal of Geomechanics, 3(1): 55-63.

[14] Kristensson, O., Ahadi, A.: 2005, Numerical study of localization in soil systems, Computers and Geotechnics, 32: 600-612.

[15] Wriggers, P., Moftah, S. O.: 2006, Mesoscale models for concrete: Homogenisation and damage behaviour, Finite Elements in Analysis and Design, 42: 623-636.

[16] ASTM D5311_92. 2007. Standard test method for load controlled cyclic triaxial strength of soil. Annual Book of ASTM Standards, 04.08, Soil and Rock (I). ASTM International, West Conshohocken, PA.

[17] De Silva, L. I. N., Koseki, J., Sato, T. and Wang, L.: 2005, High capacity hollow cylinder apparatus with local strain measurements, In Proceedings of the Second Japan-U.S. Workshop on Testing, Modeling and Simulation, Geotechnical Special Publication, ASCE, 156: 16-28.

[18] De Silva, L. I. N., Koseki, J., Sato, T., Kiyota, T. and Honda, T.: 2008, Quasi-elastic bulk modulus of sand based on volume change and local deformation measurement of hollow cylindrical specimen, In Proceedings of the 4th International Symposium on Deformation Characteristics of Geomaterials, IS-Atlanta, 2: 775-781.

[19] Ampadu, S. I. K.: 1991, Undrained behaviour of kaolin in torsional simple shear, Doctor of engineering thesis, Department of civil engineering, The University of Tokyo, Japan.

[20] Soltani-Jigheh H. and Soroush, A.: 2010, Cyclic behavior of mixed clay soils, International Journal of Civil Engineering, 8(2): 99-106.

[21] Prakasha, K.S., Chandrasekaran, V.S.: 2005, Behavior of marine sand-clay mixtures under static and cyclic triaxial shear, Journal of Geotechnical and Geoenvironmental Engineering, ASCE, 131(2): 213-222.

[22] Ni, Q., Dasari, G. R., Tan, T. S.: 2006, Equivalent granular void ratio for characterization of Singapore's Old Alluvium, Canadian Geotechnical Journal, 43: 563-573. doi:10.1139/T06-023.

[23] Rolston, J. W. and Lade, P. V.: 2009, Evaluation of practical procedure for compaction density and unit weight of rockfill material, Geotechnical Testing Journal, 32(5): 410-417.

[24] ASTM D698-07. 2007. Standard test methods for laboratory compaction characteristics of soil using standard effort. Annual Book of ASTM Standards, 04.08, Soil and Rock (I). ASTM International, West Conshohocken, PA.

[25] Ladd, R. S.: 1978, Preparing test specimens using undercompaction, Geotechnical testing journal, 1(1): 16-23.

[26] Plaxis. 2010, 2D Finite Element Code, version 2010. Plaxis bv, Delft, the Netherlands.

[27] Plaxis. 2010, 3D Finite Element Code, version 2010. Plaxis bv, Delft, the Netherlands.

[28] Brinkgreve, R. B. J., Broere, W., Waterman, D. (Editors).: 2008, Plaxis, Finite element code for soil and rock analysis, Users manual, 2D version 9.02, Rotterdam, Balkema.